RSC Advances

ROYAL SOCIETY OF CHEMISTRY

www.rsc.org/advances

Synthesis, characterization and application of core-shell magnetic molecularly imprinted polymers for selective recognition of clozapine from human serum

Jaber Javidi*[ab], Mohsen Esmaeilpour*[c], Mehdi Rajabnia Khansari [a]

[a] Department of Pharmaceutics, School of Pharmacy, Shahid Beheshti University of Medical Sciences, Tehran, Iran
[b] Students Research Committee, School of Pharmacy, Shahid Beheshti University of Medical Sciences, Tehran, Iran
[c] Chemistry Department, College of Science, Shiraz University, Shiraz, Iran

*Corresponding author. Tel.: +98 7116137738, fax: +98 7112286008.
E-mail address: jaberjavidi@sbmu.ac.ir (J. Javidi), m1250m551085@yahoo.com (M. Esmaeilpour)

Abstract

In this article, a magnetic molecularly imprinted polymer (MMIPs) based on Fe_3O_4@SiO_2 has been synthesized for simply extraction of clozapine (CLZ) from human serum. The MIPs were coated on the Fe_3O_4@SiO_2-NH_2 surface by the copolymerization of methacrylic acid with ethylene glycol dimethacrylate; and clozapine as template molecule. The properties of obtained Fe_3O_4@SiO_2-MIPs were characterized by fourier transform infrared spectroscopy, X-ray diffraction, transmission electron microscopy, scanning electron microscopy, dynamic light scattering, energy dispersive X-ray analysis (EDX), vibration sample magnetometer and rebinding experiments. The Fe_3O_4@SiO_2-MIPs showed a highly improved imprinting capacity, a fast adsorption equilibrium, and significant selectivity in molecularly imprinted solid-phase extraction of CLZ from human serum. In addition, MMIPs were regenerated and their adsorption capacity in the eighth use was about 6.67% loss in clozapine solution. Also, the intra and inter-day precision values were

less than 6 and 4%, respectively. These results suggest Fe_3O_4@SiO_2-MIPs may be used for selective extraction and analysis of CLZ in human serum.

Keywords

Core-shell magnetic nanoparticles; Molecularly imprinted polymers; Selective sorption; Clozapine; Magnetic susceptibility

1. Introduction

Molecular imprinting is a powerful technique for creating specific binding sites in molecularly imprinted polymers (MIPs) [1-4]. MIPs are obtained by the polymerization of functional monomers using a cross-linker around a template. The removal of template leaves behind recognition sites of functional and shape complementary to the template [5-7]. Compared to enzymes, antibodies, or biological molecules, MIPs show various inherent advantages such as 1) MIPs provided good physical and chemical stability; 2) MIPs can be used in harsh chemical environments without loss of binding properties; 3) Molecularly imprinted polymers (MIPs) are inexpensive to produce, reusable, and are applicable to a number of different operating conditions. Furthermore, the preparation of MIPs is quite simple and economical [7, 8]. These materials have been used for a wide variety of applications, including in the fields of catalysis [9], chemical sensors [10], food analysis [11], solid-phase extraction (SPE) [12-15], chromatography [16, 17], environmental analysis [18], pharmaceutical analysis [19] and drug controlled release [20]. MIPs have been prepared by bulk polymerization [21-24], precipitation polymerization [25-27], membrane polymerization [28, 29], multi-step swelling and polymerization [30-32] or surface-

grafting polymerization [33–35]. MIPs as SPE sorbents have attracted considerable attention for being able to selectively recognize the target molecules from a mixture of chemical species. With the development of molecular imprinted-SPE (MISPE), magnetic separation technology, in which polymers are prepared by fabricating the MIP on the surface of a magnetic substrate, has received considerable attention in recent years for its potential application in extraction and separation [36-39]. Due to the high magnetic susceptibility of magnetic nanoparticles (MNPs), magnetic molecularly imprinted polymers (MMIPs) can be easily collected and separated by an external magnetic field without additional centrifugation or filtration, which makes separation easier and faster [40].

Recently, magnetic core-shell materials, which combine features of cores and various functional shells for different applications, have gained much attention and undergone intensive investigation for their unique magnetic properties, good stability [41], biological safety [42], low cytotoxicity [43,44], chemically modifiable surface [45,46], potential applications in medicinal [47,48], environmental [49], optical [50], chemical areas [51,52] and magnetic molecularly imprinted polymer [53,54]. For this purpose, Fe_3O_4@SiO_2 nanoparticles is an excellent candidate as the supporting material because of its reactivity with various coupling agents, compatibility, reliable chemical stability, and the inherent properties of the magnetic element, which makes the resulting MIP magnetically susceptible and therefore, be easily separated by an external magnetic field after adsorption and recognition [54,55].

Clozapine is an effective antipsychotic drug treating schizophrenia with high toxicity [56]. Unlike traditional antipsychotics, clozapine has a low propensity for

extrapyramidal side effects and minimal effect on prolactin secretion. Despite its therapeutic potential, wider use of clozapine has been limited by the high risk of agranulocytosis occurring in 1–2% of the patients [57]. Several analytical methods have been described for the quantification of clozapine and its metabolites in human plasma or serum, based on a variety of detection and separation techniques. Owing to its importance, researchers used many analytical methods to study it, including capillary zone electrophoresis [58], high-performance liquid chromatography [59], spectrophotometry [60], mass spectrometry, etc. [61].

In this work, we prepared magnetic Fe_3O_4@SiO_2-MIPs with uniform core-shell structure by combining surface imprinting and nanotechniques. First, Fe_3O_4@SiO_2 nanosphere core-shell was synthesized using nano Fe_3O_4 as the core, TEOS as the silica source and PVA as the surfactant. Then, Fe_3O_4@SiO_2-NH_2 was prepared by coupling the aminosilica groups on the Fe_3O_4@SiO_2 surface through (3-aminopropyl) triethoxysilane (APTES). The MIPs were coated on the Fe_3O_4@SiO_2-NH_2 surface by the copolymerization of the amino end groups with functional monomer, methacrylic acid (MAA), using a cross-linking agent, ethylene glycol dimethacrylate (EGDMA); an initiator, azobisisobutyronitrile (AIBN); and a template molecule, clozapine.

The characterization, binding capacity, kinetics, selectivity and regeneration of these Fe_3O_4@SiO_2-MIPs particles were investigated. Finally, Fe_3O_4@SiO_2-MIPs was used as sorbent for extraction and determination of clozapine in human serum.

2. Experimental

2.1. Materials and physical measurements

Chemical reagents used in our experiments were purchased from the Merck Chemical Company and were used as received without further purification. Fourier transform infrared (FT-IR) spectra were obtained using a Shimadzu FT-IR 8300 spectrophotometer. X-ray powder diffraction (XRD) analysis was conducted on a Bruker AXS D8-advance X-ray diffractometer using Cu Kα radiation (λ= 1.5418). Scanning electron microscopy (SEM) images were obtained on Philips XL-30ESEM and transmission electron microscopy (TEM) images were obtained on a Philips EM208 transmission electron microscope with an accelerating voltage of 100 kV. The elements in the samples were probed by energy-dispersive X-ray (EDX) spectroscopy accessory to the Philips scanning electron microscopy (SEM). Magnetic characterization was carried out on a vibrating sample magnetometer (Meghnatis Daghigh Kavir Co., Iran) at room temperature and dynamic light scattering (DLS) were recorded on a HORIBA-LB550. Clozapine, diazepam, fluoxetine and phenytoin were purchased from Tehran Chemie (Tehran, Iran). The structures of chemicals used or assayed in this study are presented in Figure 1.

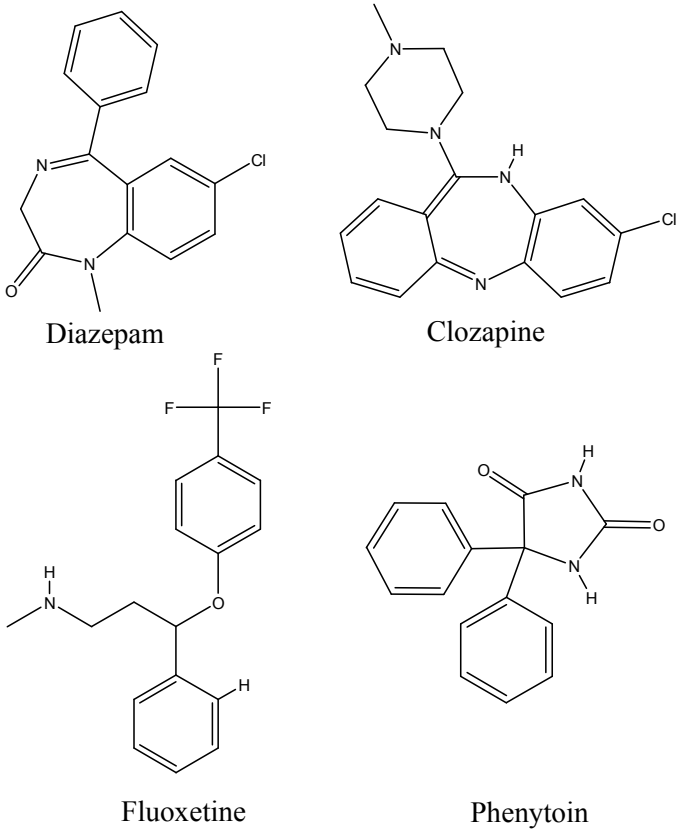

Fig. 1. Structures of the chemicals used or assayed in this study.

2.2. Preparation of standard and calibration solutions

10 mg of CLZ was dissolved in 10 mL methanol to prepare stock solution. The standard solutions (6.1, 15.3, 30.6, 61.2, 153, 306 μM) used for rebinding tests were prepared from stock solution by dilution with ACN (Acetonitrile). The standard solutions (2, 5, 10, 20, 50, 100 μgmL^{-1}) used for spiking calibration samples were prepared from the stock solution by dilution with water. 100 μL of standard solutions was added to 900 μL serum to obtain calibration standards (0.2, 0.5, 1, 2, 5, 10 μgmL^{-1}). The serum samples were frozen and stored in −20 ^{o}C.

2.3. Preparation of Fe_3O_4@SiO_2-MIPs

2.3.1. Synthesis of Fe_3O_4 NPs

The mixture of $FeCl_3 \cdot 6H_2O$ (1.3 g, 4.8 mmol) in water (15 mL) was added to the solution of polyvinyl alcohol (PVA 15000) (1 g), as a surfactant, and $FeCl_2 \cdot 4H_2O$ (0.9 g, 4.5 mmol) in water (15 mL), which was prepared by completely dissolving PVA in water followed by addition of $FeCl_2 \cdot 4H_2O$. The resultant solution was left to be stirred for 0.5 h in 80 ◦C. Then hexamethylenetetramine (HMTA) (1.0 mol/L) was added drop by drop with vigorous stirring to produce a black solid product when reaction media reaches pH 10. The resultant mixture was heated on water bath for 2 h at 60 ◦C and the black magnetite solid product was filtered and washed with ethanol three times and was then dried at 80 ◦C for 10 h [62-64].

2.3.2. Synthesis of amino-modified Fe_3O_4@SiO_2 NPs (Fe_3O_4@SiO_2-NH_2)

The core-shell Fe_3O_4@SiO_2 nanospheres were prepared by a modified Stober method [65-67]. Briefly, Fe_3O_4 (0.50 g, 2.1 mmol) was dispersed in the mixture of ethanol (50 mL), deionized water (5 mL) and tetraethoxysilane (TEOS) (0.20 mL), followed by the addition of 5.0 mL of NaOH (10 wt%). This solution was stirred mechanically for 30 min at room temperature. Then the product, Fe_3O_4@SiO_2, was separated by an external magnet, and was washed with deionized water and ethanol three times and dried at 80 ◦C for 10 h.

Then, Fe_3O_4@SiO_2 (0.5 g) was added to the solution of 3-(triethoxysilyl)-propylamine (1 mmol, 0.176 g) in ethanol (5 mL) and the resultant mixture was under reflux for 12 h under nitrogen atmosphere. After refluxing, the mixture was cooled to room

temperature, filtered by an external magnet and the product was washed with ethanol and water to remove unreacted species and dried at 80 ◦C for 6 h [68, 69].

2.3.3. Preparation of the core-shell Fe_3O_4@SiO_2-MIPs and Fe_3O_4@SiO_2-NIPs

1 g Fe_3O_4@SiO_2-NH_2, CLZ as the template and MAA as the functional monomer, were dissolved in 10 mL acetonitrile under ultrasonic vibration for 10 min, and then the mixture was placed in dark for 12 h to form a template-monomer complex. Then, EGDMA as the cross-linker, and AIBN (0.2 g) as the initiator, were added. The reaction mixture was purged with nitrogen and stirred at 60 ^{o}C for 22 h to complete radical polymerization. Then, clozapine Fe_3O_4@SiO_2-MIPs nanoparticles were obtained. After the polymerization, the obtained polymers were washed with the mixture solution of methanol/acetic acid (8:2, v/v) using soxhlet extraction to remove the template molecules. The washing was continued until no CLZ or other compound was detected in supernatant. Finally, the product (Fe_3O_4@SiO_2-MIPs) was dried in vacuum at 70 ^{o}C. Fig. 2 presents the procedure for the preparation of Fe_3O_4@SiO_2-MIPs nanoparticles stepwise.

Blank non-imprinted polymers, Fe_3O_4@SiO_2-NIPs (MNIPs), were prepared, in the absence of CLZ under the same condition as described above.

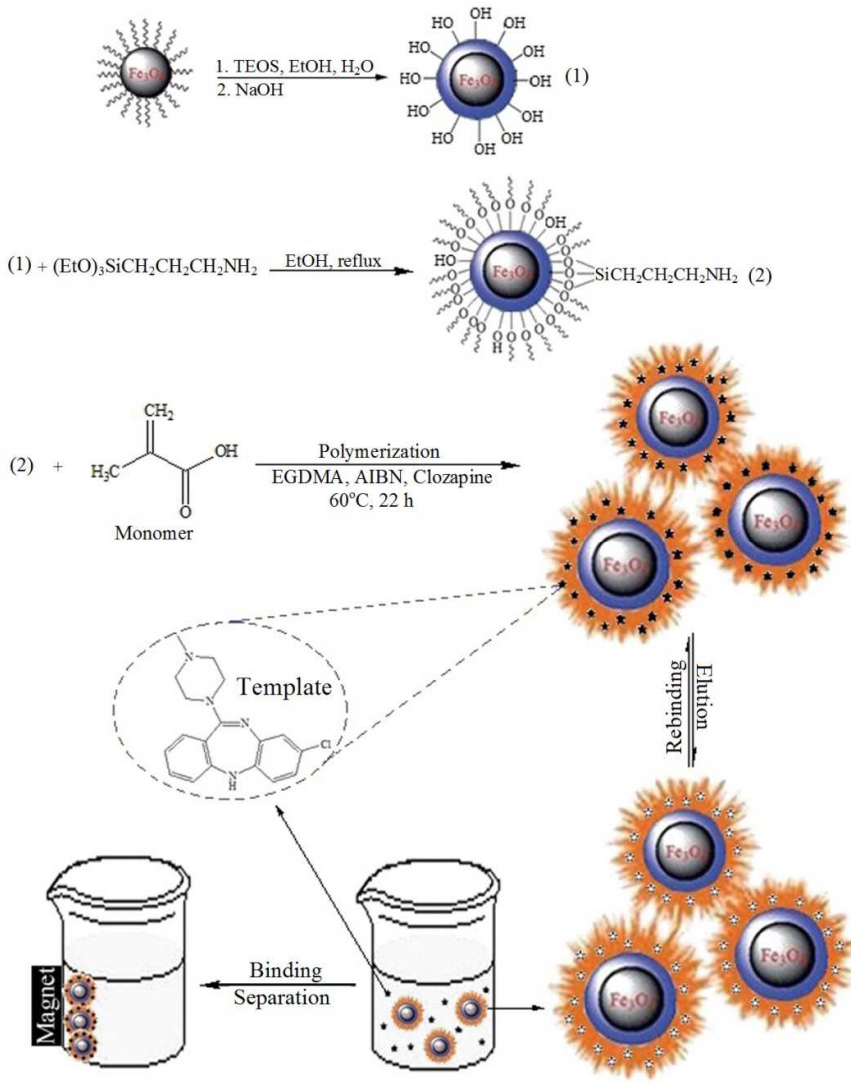

Fig. 2. Schematic representation of preparation for Fe_3O_4@SiO_2-MIPs nanoparticles.

2.4. Absorption procedure equilibrium

For evaluation of the adsorption capacity of the MMIPs, the adsorption experiment was performed. 10 mg of MMIPs or MNIPs were equilibrated with 1 mL of concentrations (20 μg/mL to 120 μg/mL) of CLZ dissolved in acetonitrile in a 2 mL centrifugal tube and shaken for 24 h at room temperature. Subsequently, the MMIPs and MNIPs were magnetically separated from the solution and supernatant was

analyzed by HPLC. The amount of bound CLZ was calculated from the difference between initial and final concentrations in solution.

The equilibrium adsorption capacity S_b (μmol/g) was calculated as Eq. (1):

$$S_b = \frac{(C_i - C_f)V}{WM} \quad (1)$$

In this equation, C_f (μg/mL) is the CLZ concentration of the supernatant solution after the adsorption, C_i (μg/mL) means the initial concentration of CLZ solution, V (mL) equals the volume of the initial CLZ solution, W (g) is the weight of the MMIPs or MNIPs and M (g/mol) is the molar mass of CLZ. Each test was carried out four times and Mean ± SD was reported.

For investigation of the selectivity of the MMIPs, three different drugs (diazepam, fluoxetine and phenytoin) with CLZ were chosen and their structures are shown in Fig. 1. 20 mg of MMIPs or MNIPs were mixed with 1 mL of 20 μg/mL solution of the studied compounds prepared in acetonitrile and then kept stirring for 24 h at room temperature. The particles were collected by a magnet. HPLC detections were applied in the supernatants of the studied solutions.

Interrelated adsorbed coefficients which including distribution coefficient and selectivity coefficient were evaluated.

The distribution coefficient was calculated according to Eq. (2):

$$k_d = \frac{C_a}{C_f} \quad (2)$$

As the concentration of the adsorbed medium, $C_a = (C_i - C_f) \times V/W$, and C_f is the free concentrations of the solution. In this equation, C_i (μg/mL), C_f (μg/mL), V (mL), and W (g) were described preciously.

Also, the selectivity coefficient (k) and Relative selectivity coefficient (k') were calculated by Eq. (3) and Eq. (4) respectively:

(3) $$k = \frac{k_{d1}}{k_{d2}}$$

(4) $$k' = \frac{k_{MMIP}}{k_{MNIP}}$$

In order to compare the selectivity of the MMIPs between CLZ and three different drugs, the selectivity coefficient (k) was calculated.

K_{d1} stands for the distribution coefficient for CLZ and k_{d2} stands for the distribution coefficients for three different drugs.

2.5. Extraction of CLZ from human serum samples

800 μL of ACN was added to 200 μL of serum in order to precipitate the serum proteins. After centrifugation (13000 rpm for 10 min), 1.5 mL deionized water was added to 500 μL of supernatant. 40 mg of MMIPs were added into the solution and shook at room temperature for 30 min. A magnet was used to separate MMIPs from the solution followed by washing the MMIPs with 1 mL of methanol/acetic acid (9:1, v/v) for 20 min. 500 μL supernatants were evaporated to dryness and dissolved in 100 μL of methanol for further HPLC–UV analysis.

3. Results and discussion

3.1. Characterization of imprinted magnetic nanoparticles

Fourier transform infrared (FT-IR) spectra for magnetic Fe_3O_4 nanoparticles (MNPs), Fe_3O_4@SiO_2, Fe_3O_4@SiO_2-NH_2, Fe_3O_4@SiO_2-MIPs and Fe_3O_4@SiO_2-NIPs nanoparticles were recorded. Some of the important bands are given in Table 1. The bands centered around 3400 cm^{-1} and 1620 cm^{-1} are, respectively, assigned to the O-H stretching and deforming vibrations of adsorbed water. For all samples, the absorption peak at 570 cm^{-1} is observed, corresponding to the Fe-O vibration from the magnetite phase [70]. The adsorption peaks at 1100 and 780 cm^{-1} corresponds to the antisymmetric and symmetricstretching vibration of Si-O-Si bond in oxygen–silica tetrahedron, respectively [70]. Evidently, it indicates that the silica has been successfully coated on the surface of superparamagnetic Fe_3O_4 NPs. At FT-IR spectrum of Fe_3O_4@SiO_2-NH_2 nanoparticles; the peaks at 569, 1091, and 1591 cm^{-1} are attributed to Fe-O (stretching vibration), Si-O-Si (asymmetric stretching) and N-H (bending), respectively. Also, the presence of several bands with medium intensity in 2861–2927 cm^{-1} and 3238–3303 regions are allocated to C–H stretching of the propyl group and N–H stretching. The strong absorption bands at around 1727 and 1260 cm^{-1}, which were assigned to C=O stretching vibration of carboxyl (MAA) and C-O symmetric stretching vibration, respectively [71]. Also, the peaks at 2930 cm^{-1} and 2990 cm^{-1} of Fe_3O_4@SiO_2-MIPs, indicated the presence of C-H stretching bands of both -CH_3 and -CH_2 groups. In addition, Fe_3O_4@SiO_2-MIPs and Fe_3O_4@SiO_2-NIPs showed almost the same characteristic absorption bands, indicating the complete

removal of templates. These results indicate the co-polymerization of MAA and EGDMA on the surface Fe_3O_4@SiO_2-NH_2 in the presence of AIBN has been initiated.

Table 1: Infrared spectroscopic data for Fe_3O_4, Fe_3O_4@SiO_2, Fe_3O_4@SiO_2-NH_2, Fe_3O_4@SiO_2-MIPs and e) Fe_3O_4@SiO_2-NIPsnanoparticles.

vibration mode assignment	Fe_3O_4 (Cm^{-1})	Fe_3O_4@SiO_2 (Cm^{-1})	Fe_3O_4@SiO_2-NH_2 (Cm^{-1})	Fe_3O_4@SiO_2-MIPs (Cm^{-1})	Fe_3O_4@SiO_2-NIPs (Cm^{-1})
Fe-O	570	571	569	570	572
Si-O-Si (symmetric)	-	789	771	776	782
Si-O-Si (asymmetric)	-	1097	1091	1109	1110
N-H	-	-	3100-3300	-	-
$\delta(CH_2)$	-	-	1472	1471	1469
C-H	-	-	2861-2927	2931-2985	2932-2989
C-O	-	-	-	1257	1260
C=O (ester)	-	-	-	1727	1728
O-H	3393	3401	3300-3400	3437	3428

Fig. 3 displays the XRD patterns of the Fe_3O_4 NPs, Fe_3O_4@-SiO_2 and Fe_3O_4@SiO_2-MIPs nanoparticles. As presented, six characteristic diffraction peaks (2Θ = 30.1, 35.4, 43.1, 53.4, 57 and 62.6◦, correspond to (220), (311), (400), (422), (511) and (440) reflections of inverse spinel Fe_3O_4 NPs, were also observed for Fe_3O_4@SiO_2 and Fe_3O_4@SiO_2-MIPs nanoparticles (reference JCPDS card no. 19-629) (Fig. 3) [68]. This revealed that the surface modification of the Fe_3O_4 nanoparticles does not lead to their phase changes. It can be seen that the Fe_3O_4 obtained has highly crystalline cubic spinel structure which agrees with the standard Fe_3O_4 (cubic phase) XRD spectrum (PDF#88-0866). From Fig. 3b, we can see the XRD pattern of Fe_3O_4@SiO_2 showing an obvious diffusion peak at 2Θ = 10-25°, generally considered as the diffusion peak of amorphous silica. For Fe_3O_4@SiO_2-MIPs nanoparticles, the broad peak was transferred to lower angles due to the synergetic effect of amorphous silica and polymer (Fig. 3c).

The broadening of each peak in XRD mean crystallite size was calculated by applying Scherrer's equation: D= $K\lambda/\beta \cos\alpha$, where K is a constant (K= 0.9 for Cu-Kα), D is the average diameter in Å, β is the broadening of the diffraction line measured at half of its maximum intensity in radians, λ is the wavelength of the X-rays and α is the Bragg diffraction angle. According to the result calculated by Scherrer equation, it was found that the diameter of Fe_3O_4 nanoparticles obtained was about 12 nm and Fe_3O_4@SiO_2 microspheres were obtained with a diameter of about 20 nm due to the agglomeration of Fe_3O_4 inside nanospheres and surface growth of silica on the shell [72].

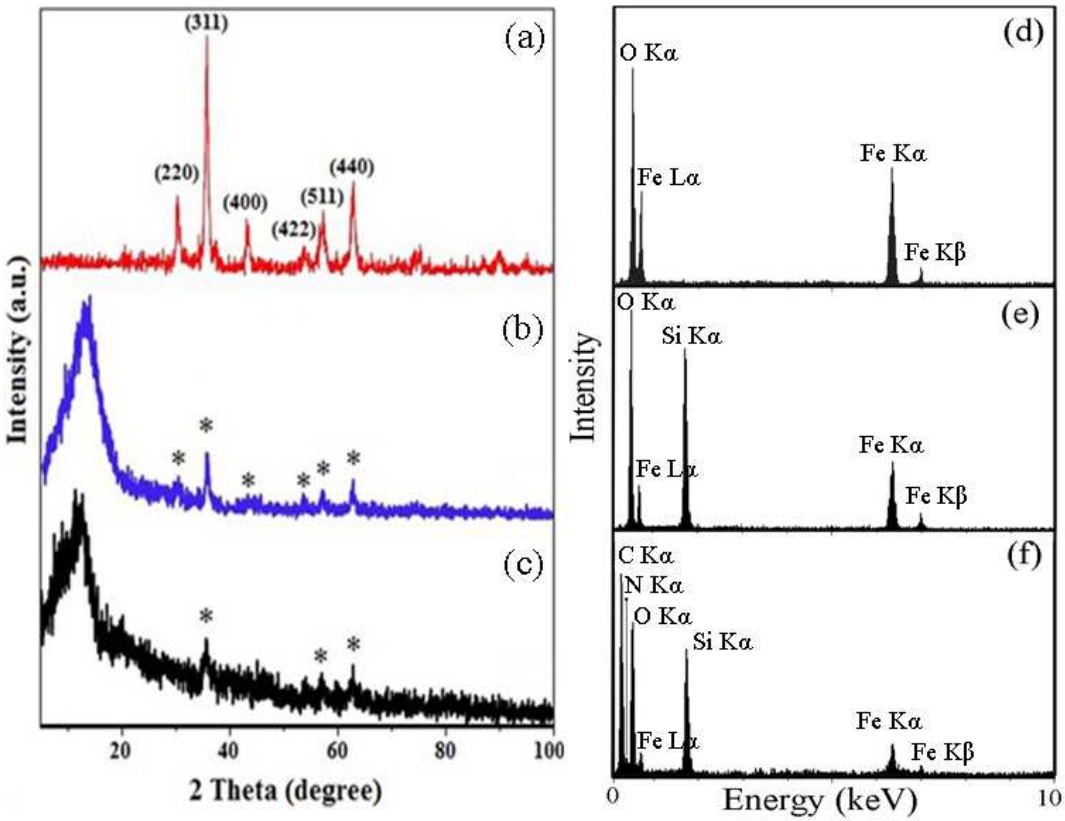

Fig. 3. XRD patterns of (a) Fe_3O_4, (b) Fe_3O_4@SiO_2 and (c) Fe_3O_4@SiO_2-MIPs nanoparticles; EDX spectra of (d) Fe_3O_4, (e) Fe_3O_4@SiO_2 and (f) Fe_3O_4@SiO_2-MIPs.

The components of the Fe_3O_4, Fe_3O_4@SiO_2 and Fe_3O_4@SiO_2-MIPs nanoparticles were analyzed using energy dispersive spectroscopy (EDS) in Fig. 3(d), (e) and (f), respectively. In Fig. 3d, the EDS spectrum of Fe_3O_4 only showed peaks of iron and oxygen. As shown in the spectra of Fe_3O_4@SiO_2 in Fig. 3e, the presence of Si, O, and Fe signals indicates that the iron oxide particles are loaded into silica, and the higher intensity of the Si peak compared with the Fe peaks indicates that the Fe_3O_4 nanoparticles were trapped by SiO_2. Fig. 3f is the EDX spectrum of the Fe_3O_4@SiO_2-MIPs nanoparticles in which Fe, O, Si, C, and N are all present. This implied that MMIPs was coated on the surface of the Fe_3O_4@SiO_2 NPs.

The morphology and sizes of (a) Fe_3O_4 and (b) Fe_3O_4@SiO_2 particles were observed by transmission electron microscopy (TEM) as shown in Fig. 4.

The mesoporous silica shell on the surface of Fe_3O_4 is quite homogeneous and exhibits good monodispersity with estimated thickness of 8 nm (Fig. 4b). The morphology of Fe_3O_4, Fe_3O_4@SiO_2 and Fe_3O_4@SiO_2-MIPs nanoparticles were also observed by SEM (Fig. 4c-e). The SEM images indicate the successful coating of themagnetic Fe_3O_4 particles. The Fe_3O_4@SiO_2-MIPs nanoparticles are approximately spherical shapes with a smooth surface morphology. The diameter of the nanoparticles is found to be approximately 100 nm and the thickness of MIP layer obtained was about 30 nm (Fig. 4e).

In this study, the hydrodynamic diameter of Fe_3O_4, Fe_3O_4@SiO_2 and Fe_3O_4@SiO_2-MIPs nanoparticles is determined by the DLS technique (Fig. 4f-h). The average diameters of particles are evaluated to be about 12 nm for Fe_3O_4 (Fig. 4f), 20 nm for Fe_3O_4@SiO_2 (Fig. 4g) and 95 nm for Fe_3O_4@SiO_2-MIPs (Fig. 4h).

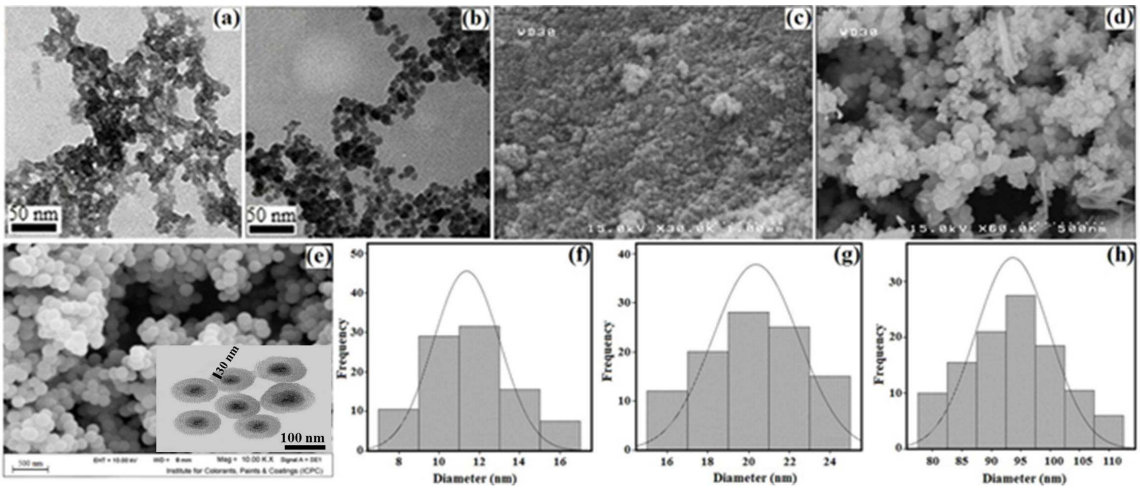

Fig. 4. TEM images of a) Fe_3O_4, b) Fe_3O_4@SiO_2 and SEM images of c) Fe_3O_4, d) Fe_3O_4@SiO_2, e) Fe_3O_4@SiO_2-MIPs and the size distributions of f) Fe_3O_4, g) Fe_3O_4@SiO_2 and h) Fe_3O_4@SiO_2-MIPs, respectively.

The histogram was proposed according to the results obtained from the XRD and TEM images.

The magnetic properties of the Fe_3O_4 NPs, Fe_3O_4@SiO_2 NPs and Fe_3O_4@SiO_2-MIPs NPs were indicated by magnetization hysteresis loops. Fig. 5 shows the absence of hysteresis phenomenon and indicates that product has superparamagnetism at room temperature.

Magnetic measurement shows that pure Fe_3O_4, Fe_3O_4@SiO_2 and Fe_3O_4@SiO_2-MIPs NPs have saturation magnetization values of 64.8, 40.3 and 27.3 emu/g, respectively. These results indicated that the magnetization of Fe_3O_4 decreased considerably with the increase of amorphous silica and polymer. Nevertheless, these Fe_3O_4@SiO_2-MIPs NPs with superparamagnetic characteristics and high magnetization values can quickly respond to the external magnetic field and quickly redisperse once the external magnetic field is removed. This result reveals that the as-prepared Fe_3O_4@SiO_2-MIPs nanoparticle exhibit good magnetic responsible.

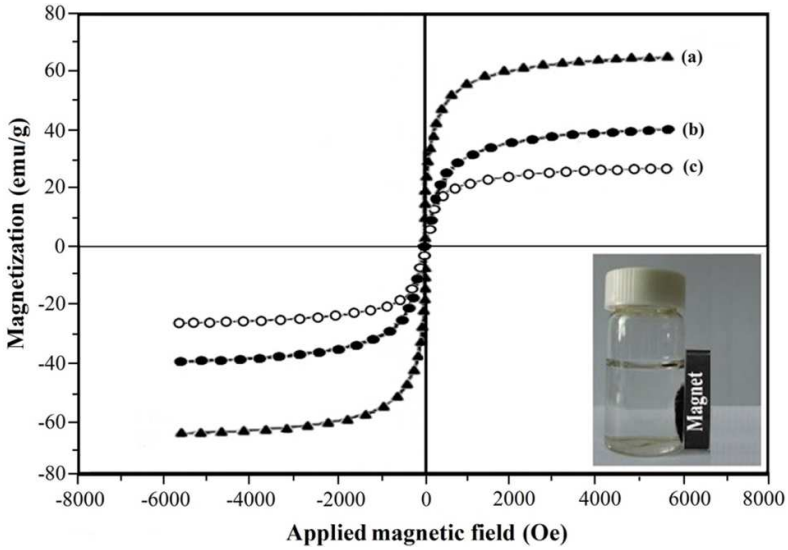

Fig. 5. Magnetization curves at 300 ^{o}K for (a) Fe_3O_4, (b) Fe_3O_4@SiO_2 and (c) Fe_3O_4@SiO_2-MIPs.

3.2. Adsorption isotherms

Scatchard analysis was shown that binding of CLZ to MMIP and its blank polymer (MNIP) was studied at different concentrations (Fig. 6). The data showed that CLZ binding to MMIP was significantly more than MNIP at all concentrations. At the beginning, both the amounts of CLZ bounded to MMIPs and MNIPs increased along the increment of initial concentrations until they reached the saturation level and then tended to be stable when the equilibrium concentration was equal or greater than 600 μM.

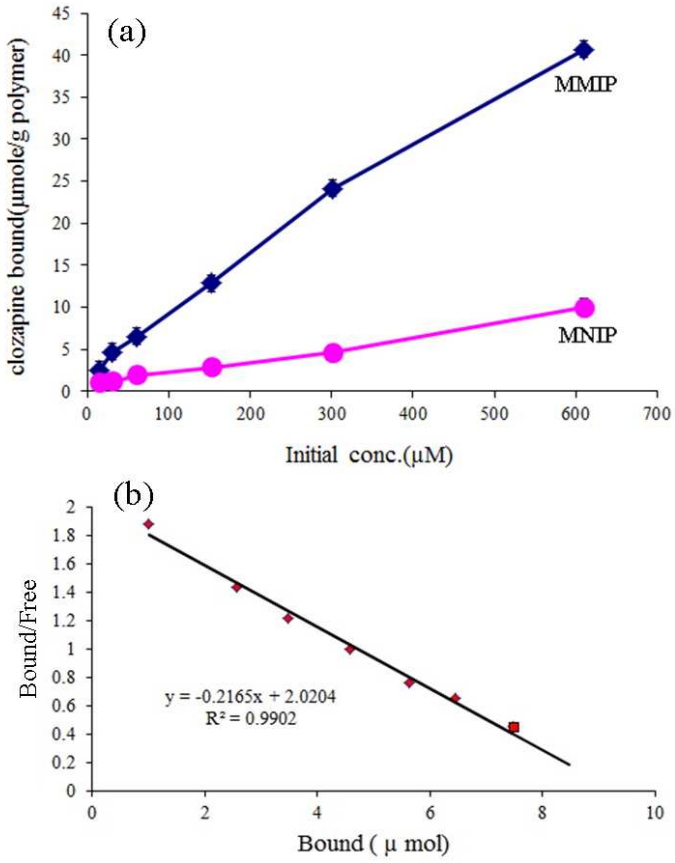

Fig. 6. (a) Adsorption isotherm of Fe_3O_4@SiO_2-MIPs and Fe_3O_4@SiO_2-NIPs using batch adsorption test (n = 6). Each point represents mean ± SD. Experiment conditions: 15 mg of polymer was incubated in 4 mL ACN with different concentrations of CLZ for 24 h at room temperature and (b) Scatchard plot to estimate the binding mechanism of Fe_3O_4@SiO_2-MIPs towards Clozapine.

Two adsorption isotherms-mathematical models, including the Langmuir and Scatchard isotherm models were used to interpret the nature of the template-polymer binding affinity and to study further on the binding properties of Fe_3O_4@SiO_2-MIPs and Fe_3O_4@SiO_2-NIPs. The results were shown in Table. 2. Interestingly, both the

Langmuir isotherm and Scatchard isotherm show the high linear correlation coefficients ($r_{Langmuir}$ =0.9789, $r_{Scatchard}$=0.9797).

In Scatchard isotherm:

$$\frac{S_b}{C} = \frac{(B_{max} - S_b)}{k_d} \quad (5)$$

Where S_b is the amount of CLZ bound to the polymers at equilibrium (mg/g), C is the free CLZ concentration at equilibrium (μg/mL), k_d is the dissociation constant (mg/L), B_{max} is the apparent maximum binding amount (mg/L). Scatchard curves were obtained by taking S_b as the x-coordinate and S_b/C as the y-coordinate. From the Scatchard plot (Fig. 6b) one dissociation constants could be discerned, one was representing high affinity binding sites with a K_d of 14.5 μM, and B_{max} of 12.78 μmol g^{-1} polymer.

Table 2. Langmuir and Scatchard isotherm constant for adsorption of CLZ on MMIPs.

Isotherm	B_{max} (μmol/g)	K_d (Lm/mol)	r^2
Scatchard isotherm	12.78	14.5	0.9797
Langmuir isotherm	10.83	11.78	0.9789

3.3. Selectivity of the MMIP

The selectivity of Fe_3O_4@SiO_2-MIPs, for CLZ was evaluated in presence of other drugs in human serum. In this part, diazepam, fluoxetine, phenytoin and CLZ were

selected as the potential interferes to investigate the selectivity of the imprinted nanoparticles based on their molecular weights and structures. The molecular recognition ability of MMIPs mainly depends on the binding ability which is closely related to the similarity between the template and the adsorbed molecules in functional groups, size and shape.

The specificity of Fe_3O_4@SiO_2-MIPs can be estimated by the imprinting factor of the selected clozapine between Fe_3O_4@SiO_2-MIPs and Fe_3O_4@SiO_2-NIPs. The imprinting factor α was determined according to Eq. (6):

$$\alpha = \frac{S_{b,MMIP}}{S_{b,MNIP}} \quad (6)$$

Where S_{bMMIP} and S_{bMNIP} are the adsorption capacity of the same analyte Fe_3O_4@MIPs and Fe_3O_4@NIPs, respectively.

As shown in Fig. 7, the Fe_3O_4@SiO_2-MIPs revealed a significantly higher adsorption amount of clozapine than other drugs; however, the Fe_3O_4@SiO_2-NIPs did not show such a difference, indicating that the template molecule had a relatively higher affinity for the imprinted polymer than other drugs. Moreover, the α amount for clozapine was also much higher than other drugs, indicating that the Fe_3O_4@SiO_2-MIPs well recognized clozapine. The differences in their spatial structures and functional groups caused a mismatch in the holes and binding sites leading to less adsorption of other drugs and an imprinting factor (α) < 1. These results indicate the excellent imprinting efficiency of the present method.

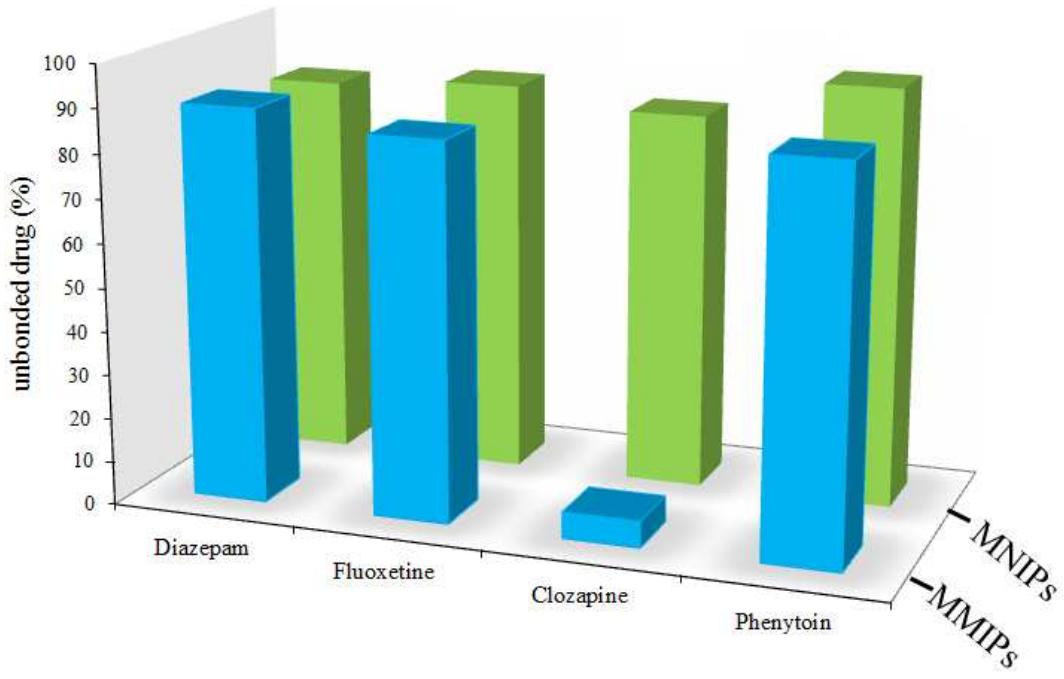

Fig. 7. Percent of unbonded drug to MMIPs and MNIPs in optimum conditions.

3.4. Optimization of extraction conditions

For evaluation the use of MMIPs to separation of clozapine in human serum samples, we investigated the parameters affecting extraction performance, including time, amount of MMIPs and temperature. The adsorption of clozapine should achieve equilibrium to allow sufficient time to obtain satisfactory recovery. The extraction times were evaluated from 5 to 90 min. The results given in Fig. 8a show an increase in recovery from 5 to 8 min and above this time a slight decrease in recovery with increasing extraction time, although the differences were not significant ($P > 0.05$). This phenomenon may be due to re-dissolution of template or formation of covalent bound between CLZ and template. We selected 8 min for extraction time, which provided 89.35% ± 1.15% recovery.

During extraction, the MMIPs were dispersed in the sample solution to rebind analyte, and we investigated the minimum amount of sorbent required for efficient recovery. MMIPs amounts from 10 to 100 mg were applied to extract clozapine from samples. The results indicated that 20 mg polymer was sufficient to yield 90.93% ± 2.53% recovery (Fig. 8b). Increasing the amount of MMIPs yielded no improvement in clozapine recovery. A slight decrease in recovery with increasing MMIPs amounts may be due to agglomeration of MMIPs nanoparticles and therefore decreasing of available site for adsorbtion of CLZ in MMIPs.

Extraction temperature was also investigated. We evaluated extraction temperature from 15 to 40 ^{o}C. The results given in Fig. 8c show a slight decrease in recovery with increasing extraction temperature above the 25 ^{o}C, although the differences were not significant ($P > 0.05$). We selected a 25 ^{o}C extraction, which provided 85.09% ± 0.78% recovery. A slight decrease in recovery with increasing temperature may be due to mobility of template. The mobility is higher at higher temperature.

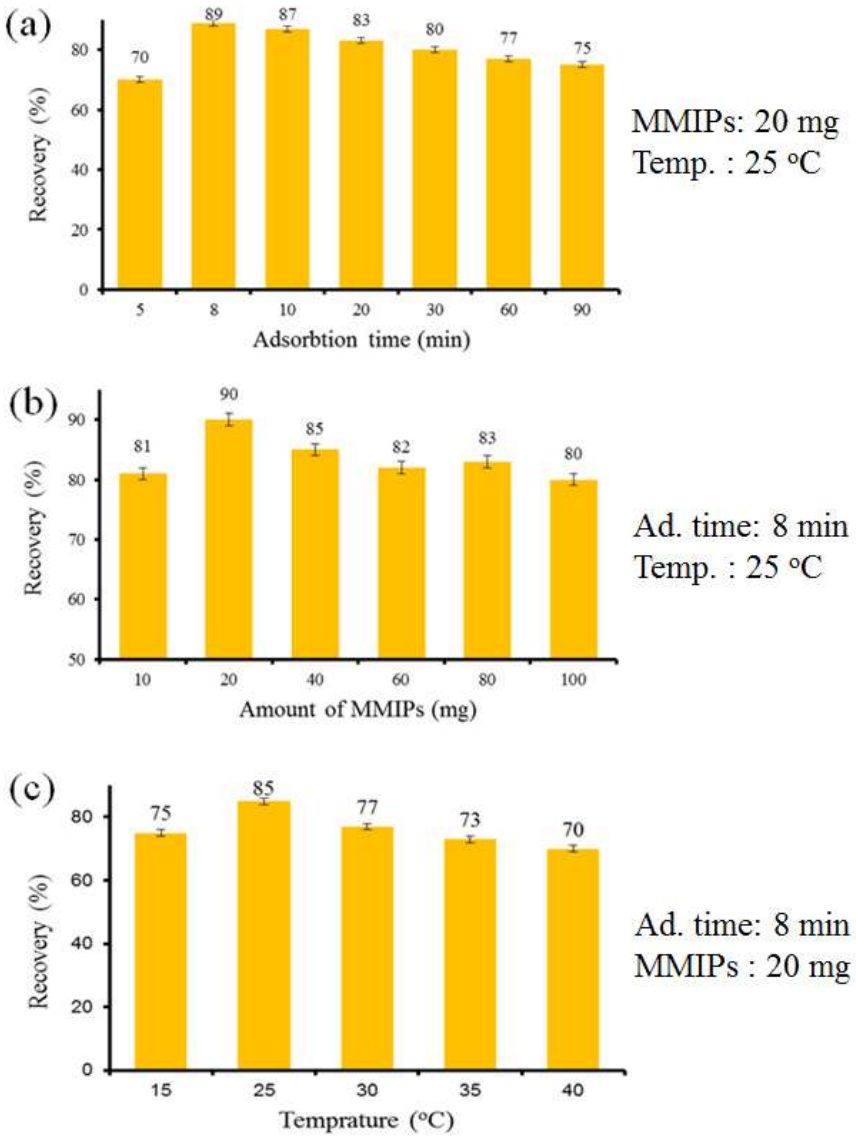

Fig. 8. Optimization of extraction conditions (a) adsorbtion time, (b) amount of MMIPs and (c) temperature.

3.5. Precision and accuracy

Intra-day and the inter-day precision and accuracy were determined by assaying blank plasma spiked with five different concentrations of clozapine. Intra-day precision was assessed by assaying five samples at three drug concentrations (50, 200 and 1000

ng/ml). Inter-day precision was evaluated by assaying (seven days) ten samples at two concentrations (100 and 500 ng/ml). In the range investigated intra-day and inter-day coefficients of variation (C.V.) were less than 6 and 4% for clozapine (Table 3).

Table 3. Intra-day and inter-day precision and accuracy of the method for clozapine.

Spiked value (ng/ml)	Measured value (ng/ml) (mean±S.D.)	Intra-day (n=5) C.V. (%)	Inter-day (n=10) C.V. (%)	Relative error (%)
50	49.56 ± 4.1	6.1		2.1
100	88.43 ± 3.7		3.4	3
200	198.13 ± 6.4	3.2		3.7
500	490.78 ± 13.67		3.6	2
1000	999.57 ± 27.02	3		0.08

3.6. Reusability

Repeated binding/removal experiments were performed to test the stability and reusability of Fe_3O_4@SiO_2-MIPs. The recovery of CLZ on Fe_3O_4@SiO_2-MIPs decreased 6.67% after eight cycles, suggesting they can be recycled**.**

4. Conclusions

In this study, Fe_3O_4@SiO_2-MIPs was synthesized with a MIPs layer on Fe_3O_4@SiO_2-NH_2 NPs with a uniform core–shell structure by surface imprinting and nanotechniques for adsorbing and recognizing of CLZ from human serum. The obtained Fe_3O_4@SiO_2-MIPs was characterized via FT-IR, XRD, TEM, SEM, DLS and VSM. The selectivity recognition properties of the Fe_3O_4@SiO_2-MIPs were evaluated and the results showed that the Fe_3O_4@SiO_2-MIPs had high adsorption capacity and selectivity for CLZ. Selectivity of the Fe_3O_4@SiO_2-MIPs procedure was investigated using CLZ and some drugs that could be present, simultaneously, in serum of patients. The prepared Fe_3O_4@SiO_2-MIPs exhibited excellently specific

recognition and saturation magnetization. Moreover, it could be easily recovered by external magnetic field, leading to a fast and selective recognition of CLZ from human serum. After Fe_3O_4@SiO_2-MIPs were reused and regenerated eight times, the adsorption capacity was still excellent. The approach reported here could provide a selective, cost-efficient and sensitive method for serum CLZ level determination in therapeutic range.

Acknowledgement

The authors are grateful to the council of Iran National Science Foundation and University of Shiraz for their unending effort to provide financial support to undertake this work.

References

[1] W. Yang, F. Jiao, L. Zhou, X. Chen and X. Jiang, *Appl. Surf. Sci.*, 2013, 284, 692.

[2] W. Liu, H. Zhao, Y. Yang, X. Liu and B. Xu, *Appl. Surf. Sci.* 2013, **277**, 146.

[3] R. Jackson, I. Petrikovics, E. P. C. Lai and J. C. C. Yu, *Anal. Methods*, 2010, **2**, 552.

[4] S. Chen, J. Chu and X. Li, *Appl. Surf. Sci.* 2013, **284**, 745.

[5] X. L. Sun, X. W. He, Y. K. Zhang and L. X. Chen, *Talanta*, 2009, **79**, 926.

[6] T. Yamazaki, S. Ohta, Y. Yanai and K.Sode, *Analytical Letters*, 2003, **36(1)**, 75.

[7] X. Su, X. Li, J. Li, M. Liu, F. Lei, X. Tan, P. Li and W. Luo. *Food Chem.* 2015, **171**, 292.

[8] C. Schirmer and H. Meisel, *Anal. Bioanal. Chem.* 2008, **392**, 223.

[9] G. Wulff, *Chem. Rev.* 2002, **102**, 1.

[10] A. L. Jenkins, R. Yin and J. L. Jensen, *Analyst,* 2001, **126**, 798.

[11] A. Molinelli, R. Weiss, B. Mizaikoff and J. Agric. *Food Chem.* 2002, **50**, 1804.

[12] S. Scorrano, L. Longo and G. Vasapollo, *Anal. Chim. Acta,* 2010, **659**, 167.

[13] F. F. Chen, R. Wang and Y. P. Shi, *Talanta*, 2012, **89**, 505.

[14] F. F. Chen, G. Y. Wang and Y. P. Shi, *J. Sep. Sci.* 2011, **34**, 2602.

[15] N. Masque, R. M. Marce and F. Borrull, *Trends Anal. Chem.*,2001, **20**, 477.

[16] B. Sellergren, *J. Chromatogr. A*, 2001, **906**, 227.

[17] K. Kim and D. Kim, *J. Appl. Polym. Sci*. 2005, **96**, 200.

[18] N. Masque, R. M. Marce, F. Borrull, P. A. G. Cormack and D. C. Sherrington, *Anal. Chem.* 2000, **72**, 4122.

[19] L. L. Zhu and X. J. Xu, *J. Chromatogr. A*, 2003, **991**, 151.

[20] S. W. Chuang, J. Rick and T. C. Chou, *Biosens. Bioelectron.* 2009, **24**, 3170.

[21] B. C. Karlsson, A. M. Rosengren, I. Näslund, P. O. Andersson and I. A. Nicholls, *J. Med. Chem.* 2010, **53**, 7932.

[22] J. He, R. Lv, J. Zhu and K. Lu, *Anal. Chim. Acta,* 2010, **66**,1215.

[23] J. Bastide, J.P. Cambon, F. Breton, S. A. Piletsky and R. Rouillon, *Anal. Chem. Acta*, 2005, **542**, 97.

[24] J. L. Urraca, M. C. Moreno-Bondi, G. Orellana, B. Sellergren and A. J. Hall, *Anal. Chem.* 2007, **79**, 4915.

[25] Y. P. Duan, C. M. Dai, Y. L. Zhang and L. Chen, *Anal. Chim.Acta*, 2013, **758**, 93.

[26] A. Prieto, S. Schrader, C. Bauer and M. Möder, *Anal. Chim.Acta*, 2011, **685**, 146.

[27] Z. Li, M. Day, J. Ding and K. Faid, *Macromolecules*, 2005, **38**, 2620.

[28] T. Alizadeh, M. R. Ganjali, M. Zare and P. Norouzi, *Food Chem.* 2012, **130**, 1108.

[29] T.A. Sergeyeva, O.A. Slinchenko, L.A. Gorbach, V.F. Matyushov, O.O. Brovko,S.A. Piletsky, L.M. Sergeeva and G.V. Elska, *Anal. Chim. Acta*, 2010, **659**, 274.

[30] Y. Watabe, K. Hosoya, N. Tanaka, T. Kubo, T. Kondo and M. Morita, *J. Polym. Sci. Part A: Polym. Sci.* 2005, **43**, 2048.

[31] H. Sanbe and J. Haginaka, *J. Pharm. Biomed. Anal.* 2003, **30**, 1835.

[32] H. Sambe, K. Hoshina, K. Hosoya and J. Haginaka, *J. Chromatogr. A*, 2006,**1134**, 16.

[33] F. Tan, D. Sun, J. Gao, Q. Zhao, X. Wang, F. Teng, X. Quan and J. Chen, *J. Hazard. Mater.* 2013, **244–245**, 750.

[34] G. Pan, Y. Zhang, X. Guo, C. Li and H. Zhang, *Biosens. Bioelectron.* 2010, **26**, 976.

[35] W. Chi, H. Shi, W. Shi, Y. Guo and T. Guo, *J. Hazard. Mater.* 2012, **227–228**, 243.

[36] L. Li, X. He, L. Chen and Y. Zhang, *Chem.Asian J.* 2009, **4**, 286.

[37] L. Xu, J. Pan, J. Dai, X. Li, H. Hang, Z. Cao and Y. Yan, *J. Hazard. Mater.* 2012, **233–234**, 48.

[38] X. Liu, D. Yu, Y. Yu and S. Ji. *Appl. Surf. Sci*., 2014, **320**, 138.

[39] Y. Hiratsuka, N. Funaya, H. Matsunaga and J. Haginaka, *J. Pharm. Biomed. Anal.* 2013, **75**, 180.

[40] J. Pan, L. C. Xu, J. Dai, X. Li, H. Hang, P. Huo, C. Li and Y. Yan. *Chem. Eng. J*, 2011, **174**, 68.

[41] S. Abramson, W. Safraou, B. Malezieux, V. Dupuis, S. Borensztajn, E. Briot, A.Bée, *J. Colloid Interface Sci.* 2011, **364**, 324.
[42] M. F. Shao, F. Y. Ning, J. W. Zhao, M. Wei, D. G. Evans, X. Duan, *J. Am. Chem. Soc.* 2012, **134**, 1071.

[43] H. X. Wu, L. H. Tang, L. An, X. Wang, H. Q. Zhang, J. L. Shi, S. P. Yang, *React. Funct.Polym.* 2012, **72**, 329.

[44] J. Liu, B. Wang, S. B. Hartono, T. T. Liu, P. Kantharidis, A. P. J. Middelberg, G. Q. Lu, L. Z. He and S. Z. Qiao, *Biomaterials*, 2012, **33**, 970.
[45] A. H. Lu, E. L. Salabas, F. Schuth, *Angew. Chem. Int. Ed.* 2007, **46**, 1222.

[46] F. H. Chen, Q. Gao and J. Z. Ni, *Nanotechnology* 2008, **19**, 165103.

[47] S. H. Xuan, S. F. Lee, J. T. F. Lau, X. M. Zhu, Y. X. J. Wang and F. Wang, *Appl. Mater. Inter.* 2012, **4**, 2033.

[48] J. Zhang, W. Sun, L. Bergman, J. M. Rosenholm, M. Lindén, G.Wu, H. Xu and H.C. Gu, *Mater. Lett.* 2012, **67**, 379.

[49] Y. H. Deng, D. W. Qi, C. H. Deng, X. M. Zhang and D. Y. Zhao, *J. Am. Chem. Soc.* 2008, **130**, 28.

[50] B. Liu, W. X. Xie, D. P. Wang, W. H. Huang, M. J. Yu and A. H. Yao, *Mater Lett.* 2008, 62, 3014.
[51] Y. H. Deng, Y. Cai, Z. K. Sun, J. Liu, C. Liu, J. Wei, W. Li, Y. Wang, D. Y. Zhao, *J. Am.Chem. Soc.* 2010, **132**, 8466.

[52] B. Panella, A. Vargas and A. Baiker, *J. Catal.* 2009, **261**, 88–93.

[53] F. F. Chen, X.Y. Xie, Y.P. Shi. *J. Chromatogr. A,* 2013, **1300**, 112.

[54] C. Hu, J. Deng, Y. Zhao, L. Xia, K. Huang, S. Ju and N. Xiao. *Food Chem*. 2014, **158**, 366.

[55] X. Kong, R. Gao, X. He, L. Chen and Y. Zhang, *J. Chromatogr. A*, 2012, **1245**, 8.
[56] T. Sharma, C. Hughes, W. Soni and V. Kumari. *Psychopharmacology,* 2003, **169**, 398.
[57] J. M. Alvir, J. A. Lieberman, A. Z. Safferman, J. L. Schwimmer and J. A. Schaff. *New Engl. J. Med.*, 1993, **329**, 162.
[58] W.R. Jin, Q. Xu and W. Li. *Electrophoresis*, 2000, **21**, 1415.

[59] Y.L. Shen, H.L. Wu, W.K. Ko and S.M. Wu. *Anal. Chim. Acta*, 2002, **460**, 201.
[60] C.S.P. Sastry, T.V. Rekha and A. Satyanarayana. *Microchim. Acta*, 1998, **128**, 201.

[61] M. Kollroser and C. Schober. *Rapid Commun. Mass. Spectrom.*, 2002, **16**, 1266.

[62] M. Esmaeilpour, J. Javidi, F. Dehghani and F. Nowroozi Dodeji, *RSC Adv.*, 2015, **5**, 26625.

[63] J. Jaber and E. Mohsen, *Colloids Surf., B*, 2013, **102**, 265.

[64] M. Esmaeilpour, A. R. Sardarian and J. Javidi, *J. Organomet. Chem.*, 2014, **749**, 233.
[65] M. Esmaeilpour, J. Javidi and M. Zandi, *Mater. Res. Bull.*, 2014, **55**, 78.
[66] J. Javidi, M. Esmaeilpour and F. Nowroozi Dodeji. *RSC Adv.*, 2015, **5**, 308.

[67] M. Esmaeilpour, J. Javidi, F. Dehghani and F. Nowroozi Dodeji, *New J. Chem.,* 2014, **38**, 5453.

[68] M. Esmaeilpour, J. Javidi, F. Nowroozi Dodeji and M. Mokhtari Abarghoui, *J. Mol. Catal. A: Chem.*, 2014, **393**, 18.

[69] M. Esmaeilpour, J. Javidi, F. Nowroozi Dodeji and M. Mokhtari Abarghoui, *Transition Met. Chem.*, 2014, **39**, 797.

[70] (a) C. Yang, J. Wu and Y. Hou, *Chem. Commun.* 2011, **47**, 5130, (b) M. Salavati-Niasari, J. Javidi and M. Dadkhah, *Com. Chem. High T. Scr. 2013,* **16 (6)**, 458.
[71] K. Yoshimatsu, K. Reimhult, A. Krozer, K. Mosbach, K. Sode and L. Ye, *Anal.Chim.Acta*, 2007, **584**, 112.
[72] M. Esmaeilpour, A. R. Sardarian and J. Javidi, *Appl. Catal., A*, 2012, **445–446**, 359.